3.4/4.0

.

You did noo assign uncertainties to the individual channel cou

Lab 5: Mössbauer Spectroscopy of Fe-57

Diego Garza (Lab Partner: Lara Braverman)

March 11, 2022

1 Background

In the absence of any external effects, the energy difference between the $I = 1/2$ and $I = 3/2$ nuclear states of ^{57}Fe is 14.4 keV. However, the local environment in which the nucleus is sitting can cause this 'true' energy difference to change. For example, chemical isomer shifts can come about when the orbital electrons of the host and neighboring atoms cause fields that can cause energy levels in the nucleus to change. Another local environment variable that can cause the nucleus to have different energy shifts when going from $I = 1/2$ to $I = 3/2$ is the nuclear Zeeman splitting effect, where one transition energy has many transition energies. Also, an electric field gradient that is due to simply the molecular structure around the nucleus of ^{57}Fe can cause a quadrupole splitting effect. To study these very fine differences in the 'true' shift in energy, we can use Mossbauer spectroscopy.

The ^{57}Fe source will emit a gamma ray in 14.4 keV, and we can use absorbers with different environments to alter how the energy shift is detected. Using a linear motor, we can move the source of gamma rays Towards and away - om the absorber, causing a Doppler effect. To look at the absorption of the Doppler-shifted gamma rays as a function of energy, we can measure the amount transmitted through a given absorber. For some fixed time t_{dwell}, the UCS-30 software can count the amount of gamma rays that pass through the absorber in a revolution of the linear motor. The software sweeps over each channel, and assigns a small time interval. It then counts the amount of gamma rays having passed in that small time interval for that channel. It keeps counting the gamma rays for all 512 channels, which will correspond to the t_{dwell}.

Using the geometry of the Michelson interferometer, we can map each fringe amount with some change in position of the linear motor over some time interval it takes for the linear motor to move. Having some change in position over a time interval, we have a velocity! We can take a fringe spectrum and map it onto a velocity spectrum. Knowing the energy shift difference due to the Doppler effect, we know $E_t' - E_t = \Delta(E(ch)) = v(ch)E_t/c$, so we can also map the velocity onto the shift in energy from the transition energy. With these different mappings and conversions, we can plot the transmission through the absorber as a function of the change in the 'true' energy transition of 14.4 keV as a linear motor moves the ^{57}Fe source. We can fit dips in the transmission energy to a known distribution and calculate some interesting characteristics about the local environment causing the shift in the energy transition. We can compare these characteristics to literature values as a check on the entire process.

To measure the chemical isomer shift, we use a stainless steel 302 absorber. To measure the shift due to the nuclear zeeman splitting effect, we take an enriched ^{57}Fe plate as the absorber. To study the shift due to an electric field gradient, we use a sodium nitroprusside absorber.

2 Velocity Calibration

To calibrate the velocity, we can first look at the fringe and make a fit to the data using Equation 1 for the fringe count

$$n(ch) = n_0|ch - ch_0| \tag{1}$$

where n_0 and ch_0 are fitted values for the slope and where the fringe goes to zero respectively. We take a fringe spectrum before and after the experiment (represented in the following Figures as "Pre" and "Post") to confirm that our conversions for the shift from the energy transition is the same throughout the experiment.

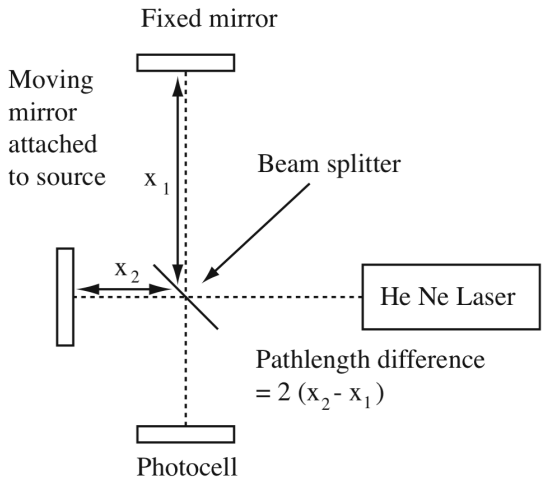

Figure 1: Michelson Interferometer Setup for Velocity Calibration

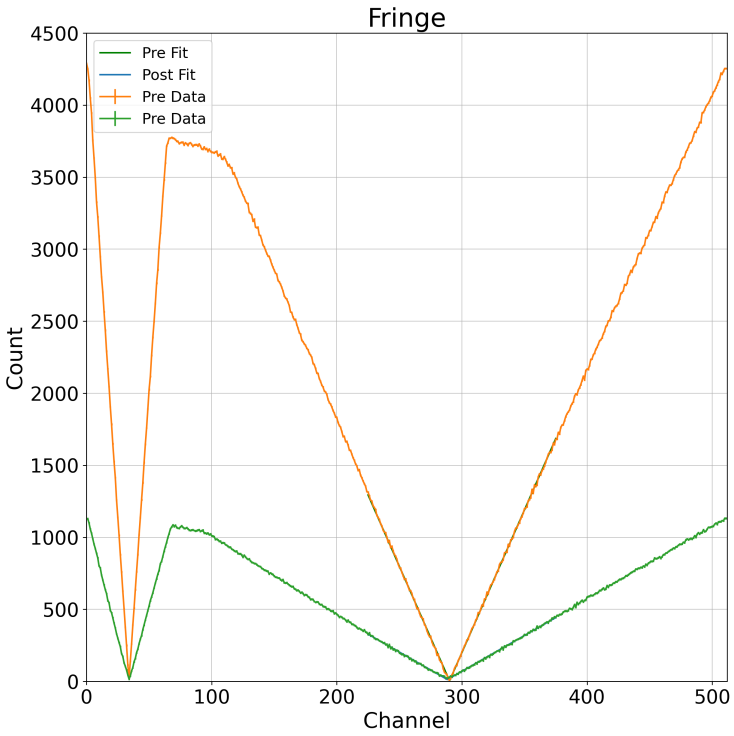

Figure 2: Fringe Fitting

Using the geometry of the Michelson Interferometer setup, we can note that the photocell will notice n fringes if $\Delta x = n\lambda/2$, where λ is the wavelength of the He Ne Laser, and Δx is the change in x_2 in Figure 1. The wavelength is given as $\lambda = 632.8$ nm.

The fitting values to the equation for the fringe values are in Table 1.

	n_0 (count/channel)	ch_0 (channel)	χ^2/N
Pre	19.81 ± 0.03	290.11 ± 0.03	2.28
Post	4.97 ± 0.03	288.41 ± 0.12	0.63

Table 1: Fitting Parameters for Fringe

With low reduced χ^2 values and Figure 2 showing the fits landing generally on top of the data, this indicates a pretty good fit to the equation. We estimated the error for the fringe count as 7 counts.

Over some region of time, we can convert the fringe counts to a velocity of the source as

$$v = \frac{\Delta x}{\Delta t} = \frac{n(ch)\lambda}{2\Delta t} = \frac{\lambda}{2\Delta t} n_0(ch - ch_0) \tag{2}$$

where Δt is the total amount of time passed after p number of revolutions of the motor. We define the region of time as some range of channels where the V shape is well defined, which here is channels 225 to 375. In total, $\Delta t = p \cdot t_{dwell}$, and we have set $t_{dwell} = 300\mu$s in the software. Recording the amount of passes, we can calculate the source's velocity.

After completing the conversion, we get Figure 3.

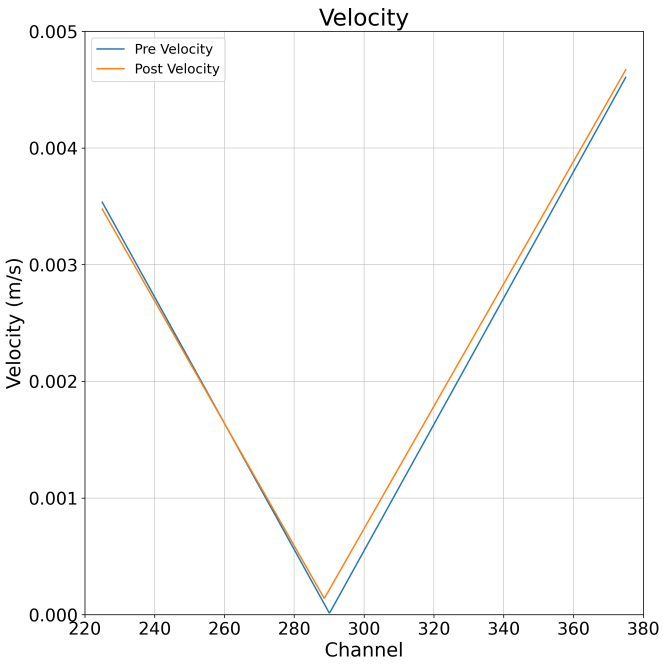

Figure 3: Velocity as a Function of Channel

Here we can see that the velocities have very similar slopes and x-axis intercepts, which gives an indication that we can use either one to convert to shifts from the transition energy. Since we calculated the velocity as a function of n_0, ch_0, and ch, we know that each of these values have some intrinsic uncertainty attributed to each. At the level of sensitivity we are interested in, we can assume that the

wavelength of the laser and the total time interval, Δt, have negligible uncertainty. In effect, we can estimate the uncertainty in the velocity of the source as Equation 3.

$$\frac{dv}{v} = \sqrt{\frac{dn_0}{n_0}^2 + \frac{dch}{(ch - ch_0)}^2 + \frac{dch_0}{(ch - ch_0)}^2} \tag{3}$$

where n_0, ch_0, dn_0 and dch_0 come from the fitting algorithm. Now we have the value for the velocity as well as its uncertainty, as a function of the channel and the channel's uncertainty.

Furthermore, we can convert this velocity value for the source, to energy shifts from the transition energy of 14.4 keV by using Equation 4.

$$\Delta E(ch) = v(ch)E_t/c \tag{4}$$

where E_t is the transition energy of 14.4 keV from the Co-57's decay to Fe-57, specifically the transition of Fe-57 $I = 1/2$ to $I = 3/2$, and c is the speed of light. Here, we take the uncertainty in the speed of light and the energy transition to be negligible. In effect, we estimate the uncertainty in this change from the true energy shift as Equation 5.

$$\Delta(\Delta E(ch)) = \Delta E(ch) \cdot dv/v \tag{5}$$

We can now create a conversion factor of channels to energy shift, taking into account the velocity as actually negative in the channels before the velocity hits zero. After plugging in the fitted values for the original fit to the fringe function given by Equation 1, we find the energy described as

$$\Delta E(ch) \pm \Delta(\Delta E(ch)) = \Delta E(ch) \pm \Delta E(ch) dv/v = \Delta E(ch)(1 \pm dv/v)$$

where we can use the fitted values and their uncertainties from Table 1 to find an equation as a function of the channel measured and its uncertainty. We can make a linear fit to this relationship to find a slope of 2.598 ± 0.003 in units of nano-eV/channels, which can be used as a conversion when the ch_0 is not important.

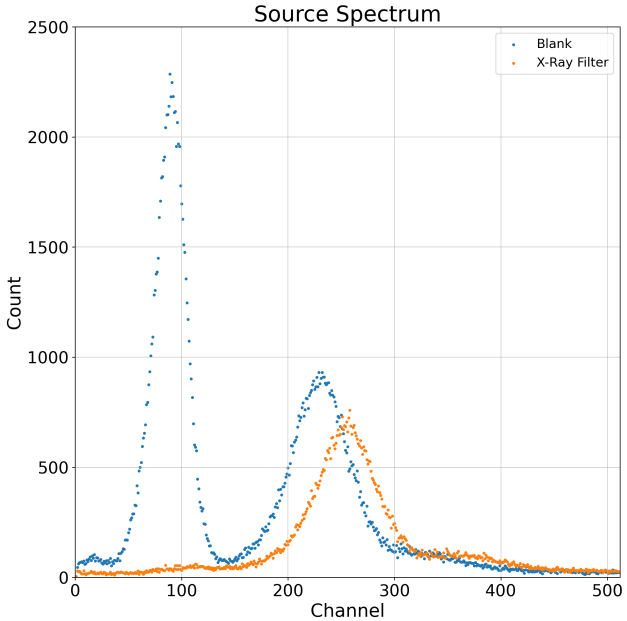

Figure 4: Source Spectrum

Before taking any spectra for the sensitive shifts in energy, we completed a spectrum of the source with and without an x-ray absorber.

The x-ray absorber can filter out the low 6 keV energy peak that is present due to its K-line emission, and help concentrate the 14.4 keV energy peak due to the energy transition.

3 Stainless Steel 302 Spectrum

To study the change to the 'true' transition energy of 14.4 keV due to a chemical isomer shift, we use a stainless steel 302 plate as an absorber for the gamma rays emitted in the transition.

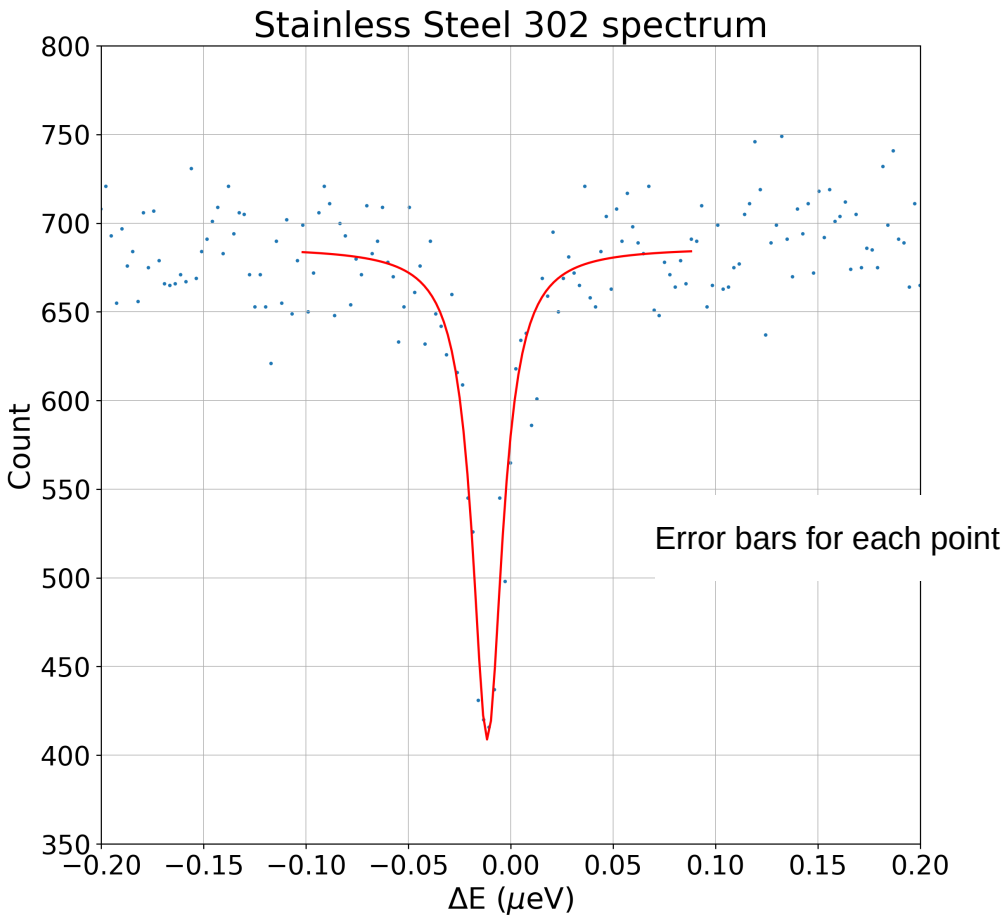

Figure 5: Stainless Steel 302 Spectrum

We know that the distribution of the absorption peaks will be Lorentzian, so we can fit a function of the form $Count = D - I(E)$, where I is a Lorentzian fitted to the spectrum and D is some constant. The Lorentzian distribution is shown in Equation 6. To choose the region of interest to fit the Lorentzian distribution, I wanted to find a region that allowed for a bit of the flat count around 700.

$$I(E) = I_0 \frac{(\Gamma/2)^2}{(E - E_0)^2 + (\Gamma/2)^2} \tag{6}$$

Here, the ΔE we want is Equation 6's E_0, and the FWHM of the distribution is Equation 6's gamma. The E_0 will provide the shift in energy where the absorption peaks, while the FWHM will provide the natural linewidth of the transition. After completing the fit, we find the final parameters are shown in Table 2.

Γ (μeV)	ΔE (μeV)	χ^2/N
0.018 +/- 0.002	-0.0116 +/- 0.0005	0.91

Table 2: Fitting Parameters for Stainless Steel Spectra

The fits were made using raw channels, so the appropriate ΔE and its uncertainty comes from Equations 4 and 5. The Γ is also fitted using channels, and since we are taking the difference between two channel values, the ch_0 end up canceling out from both sides of where the width is at half max, so we can use the slope for the conversion between channels to energy of $m = 2.598 \pm 0.003$ in units of nano-eV/channels multiplied by the channel number.

$$\Gamma = m\Gamma_{ch} \tag{7}$$

Where Γ_{ch} is the fitted FWHM when using channels. In effect, the uncertainty can be estimated as Equation 8.

$$\frac{d\Gamma}{\Gamma} = \sqrt{(\frac{d\Gamma_{ch}}{\Gamma_{ch}})^2 + (\frac{dm}{m})^2} \tag{8}$$

where we get the uncertainty in Γ_{ch} from the fitting algorithm, provided in Table 2.

Calculating the mean lifetime of the $I = 3/2$ state from $(\Gamma/2)\tau = \hbar/2$, where Gamma is half of the observed FWHM, we can isolate the mean lifetime to get Equation 9

$$\tau = \hbar/(\Gamma_{obs}/2) \tag{9}$$

We then get 71.44 ± 5.95 ns as the mean lifetime, which is about half of the literature value of 141.4 ± 1.4 ns.

We can estimate the uncertainty in $\hbar$ as negligible in this equation as it is a well-known value. In effect, the uncertainty for the mean lifetime is estimated as

$$\frac{d\tau}{\tau} = \sqrt{(\frac{d\Gamma}{\Gamma})^2} = \frac{d\Gamma}{\Gamma}$$

4 Enriched Iron Spectrum

To study the change to the 'true' transition energy of 14.4 keV due to the Zeeman effect, we use an enriched ^{57}Fe plate as an absorber for the gamma rays emitted in the transition.

Similarly as for the stainless steel, we can fit Lorentzian distributions for each peak. Also, we can find how the energy transitions are distributed from Figure 7. Each Nuclear Zeeman split can be attributed to each peak from left to right.

Since the shift in energy and velocity are linearly dependent, then each transition can still be read from low velocity / low energy shift to high velocity / high energy shift from left to right in Figure 7.

Each transition can have a change of the initial quantum number m_I equal to -1, 0, and 1. From left to right in Figure 6, the first transition is from $m_I = 1/2$ to $m_I = 3/2$, the second is $m_I = 1/2$ to $m_I = 1/2$, the third is from $m_I = 1/2$ to $m_I = -1/2$, the fourth is from $m_I = -1/2$ to $m_I = +1/2$, the fifth is from $m_I = -1/2$ to $m_I = -1/2$, and the final transition is from $m_I = -1/2$ to $m_I = -3/2$.

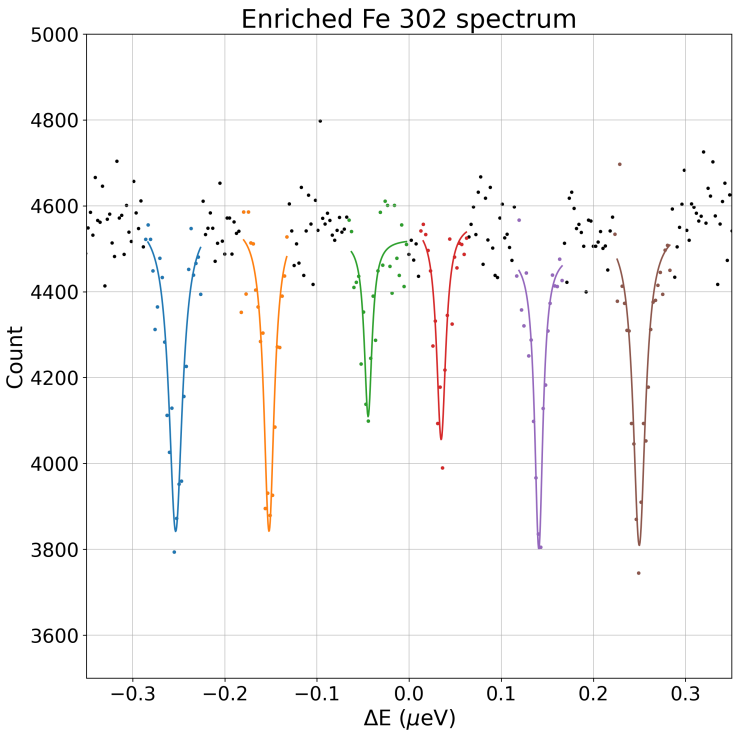

same

Figure 6: Enriched Iron Spectrum

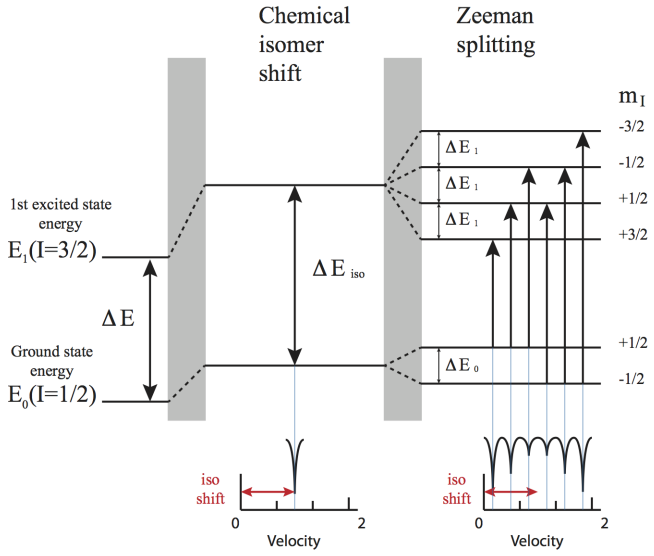

Figure 7: Zeeman Shifts

Each of these peaks had a Lorentzian distribution fitted to them, with the relevant values found in Table 3.

The uncertainties for Γ, ΔE, and τ use the same system as for the stainless steel. We can see that, as expected, most Γ are narrower than that of the observed stainless steel 0.018 ± 0.002 μeV.

Your uncertainties in deltaE are way too low because you did not assign the corr

Initial m_I	Final m_I	Γ (μeV)	ΔE (μeV)	χ^2/N	τ (ns)
+1/2	+3/2	0.019 ± 0.002	-0.2531 ± 0.0006	1.73	68.63 +/- 5.49
+1/2	+1/2	0.015 ± 0.002	-0.1515 ± 0.0005	1.57	86.90 +/- 8.80
+1/2	-1/2	0.011 ± 0.002	-0.0454 ± 0.0007	1.46	119.59 ± 16.67
-1/2	-3/2	0.013 ± 0.002	0.0344 ± 0.0006	1.17	98.31 ± 11.26
-1/2	-1/2	0.012 ± 0.002	0.1406 ± 0.0005	0.82	109.56 ± 13.99
-1/2	+1/2	0.017 ± 0.002	0.2494 ± 0.0006	1.35	75.67 ± 6.67

Table 3: Fitting Parameters for Enriched Iron Spectra

Using Figure 7, we can find ΔE_0 as the difference between energy shifts that start on different m_I values in the $I = 1/2$ state, but end up on the same m_I values in the $I = 3/2$ states. This means that either the difference between the fourth and second transition or the difference between the fifth and third transition can be used to find ΔE_0.

The first method yields 0.0186 ± 0.001 μeV, while the latter has the value 0.0186 ± 0.001 μeV. These values are in agreement with each other, which is a good check. Since we are subtracting the values, the uncertainty for these differences is given by Equation 10.

$$\Delta(\Delta E_0) = \sqrt{\Delta E_2^2 + \Delta E_1^2} \tag{10}$$

where ΔE_i are the shifts in energy peaks.

Using the relationship given by equation 9 from the wiki, we know there is a relationship between ΔE_0 and H. So we can manipulate the equation to find this magnetic field H in Equation 11.

$$H = I_0 \frac{\Delta E_0}{\mu_0} \tag{11}$$

With $I_0 = 1/2$ and $\mu_0 = 2.884 \cdot 10^{-9}$ eV/T, we can find two values of the magnitude of the magnetic field using the two values found for ΔE_0. To propagate uncertainty for the magnetic field's magnitude, we Equation 12.

$$dH = H\sqrt{\frac{\Delta(\Delta E_0)}{\Delta E_0}^2 + \frac{d\mu_0}{\mu_0}^2} \tag{12}$$

In this case, we take $d\mu_0$ to be the wiki value of $0.00007\mu_n$.

Following these steps, we get two values for the magnetic field. One for the transition difference in energy from the fourth and second transition, $H_1 = 32.68 \pm 0.14$ T, and another from the fifth and third transition $H_2 = 32.69 \pm 0.15$ T. Using these values and their appropriate uncertainty, we can fit a horizontal line that's independent of the x-value using the uncertainty to compute a weighted average to find what average value the two values provide. The averaged magnetic field found is $H_{avg} = 32.69 \pm 0.10$ T.

Both the individual and averaged values are in agreement with each other, as well as in agreement with the literature value of 33.3 ± 1.0 Tesla.

From Figure 7, we can also find the values for ΔE_1 by taking the energy shift difference between neighboring values of first and second, second and third, fifth and fourth, and fifth and sixth peaks. In that same order, we find the values for the difference between the changes from the energy shift as 0.102 ± 0.001, 0.106 ± 0.001, 0.106 ± 0.001, and 0.109 ± 0.001 in units of μeV. We can now use the similar relationship of μ_0 from the previous equation for the magnetic field, but now for μ_1 such that it follows Equation 13.

$$\mu_1 = \Delta E_1 I_1 / H \tag{13}$$

where $I_1 = 3/2$ and H is the same magnetic field found as before. The three values for the magnetic field are very close to each other, but I use the averaged magnetic field H_{avg}, as well as its associated uncertainty to complete this calculation. The uncertainty is then described in Equation 14.

$$d\mu_1 = \mu_1 \sqrt{\frac{\Delta(\Delta E_1)}{\Delta E_1}^2 + \frac{dH_{avg}}{H_{avg}}^2} \tag{14}$$

where $\Delta(\Delta E_1)$ is the uncertainty in the difference of two energy shifts, as described in equation 10. The uncertainty in the ratio of μ_0 to μ_1 is described by Equation 15.

$$d(\frac{\mu_0}{\mu_1}) = \frac{\mu_0}{\mu_1} \sqrt{\frac{d\mu_0}{\mu_0}^2 + \frac{d\mu_1}{\mu_1}^2} \tag{15}$$

Since we have four neighboring differences in energy shifts for ΔE_1, we get four different ratios. In the same order as before, reading the relevant differences from left to right, we get the following values 0.610 ± 0.005, 0.584 ± 0.005, 0.584 ± 0.005, and 0.570 ± 0.003. Two fall within uncertainty of the literature value of 0.587 ± 0.032.

Fitting similarly as for the magnetic field to a constant mu ratio value independent of x, we find a weighted average of the mu ratios as $\mu_{avg} = 0.585 \pm 0.002$.

5 Quadrupole Spectrum

To study the change to the 'true' transition energy of 14.4 keV due to quadrupole splitting, we use a sodium nitroprusside absorber plate as an absorber for the gamma rays emitted in the transition.

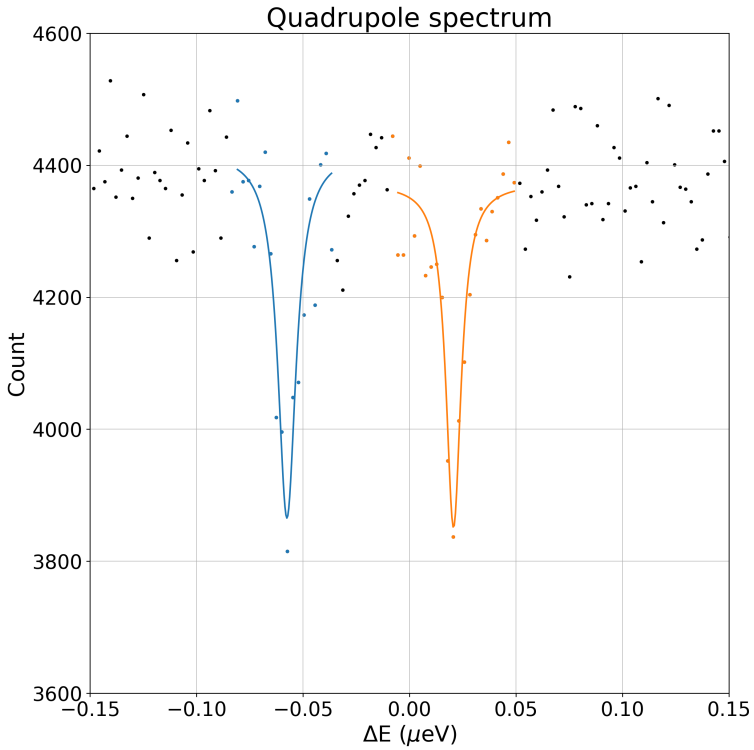

Figure 8: Quadrupole Spectrum

Similarly as for both the stainless steel and enriched iron spectra, we can fit Lorentzian distributions for each peak. Also, we can find how the energy transitions are distributed from Figure 9. Each quadrupole split can be attributed to each peak from left to right.

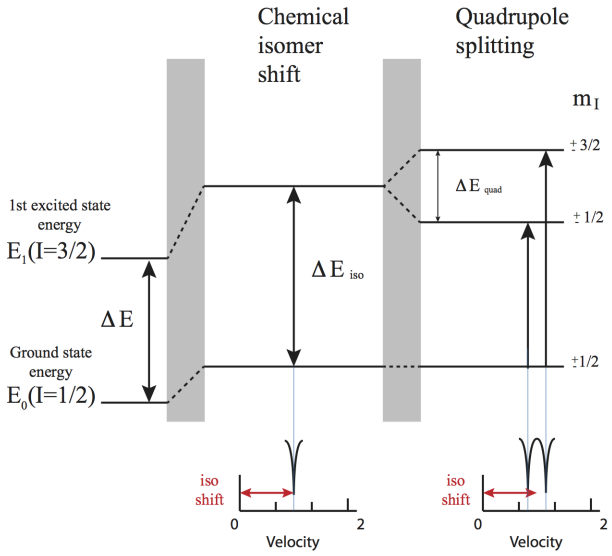

Figure 9: Quadrupole Shifts

Using a similar logic as before, we know that the lower velocity shift corresponds to a final m_I state of $\pm 1/2$, and this lower velocity can be attributed to a lower change from the 'true' energy shift. So this peak corresponds to the blue line in Figure 8, while the peak in orange corresponds to the final state of $m_I = \pm 3/2$.

Both peaks had a Lorentzian distribution fitted to them and the relevant parameters can be seen in Table 4.

Initial m_I	Final m_I	Γ (μeV)	ΔE (μeV)	χ^2/N	τ (ns)
$\pm 1/2$	$\pm 1/2$	0.012 $\pm$ 0.002	-0.0574 $\pm$ 0.0005	1.64	113.49 $\pm$ 15.01
$\pm 1/2$	$\pm 3/2$	0.009 $\pm$ 0.002	0.0205 $\pm$ 0.0005	0.75	139.96 $\pm$ 22.83

Table 4: Fitting Parameters for Sodium Nitroprusside Spectra

Taking the difference between the two energy shifts and propagating the errors like in Equation 10, we get $\Delta E_{quad} = 0.078 \pm 0.002$ μeV.

We can find an estimate for the electric field gradient by evaluating Equation 16.

$$\Delta E_{quad} = \Delta E(I = 3/2, m_I = \pm 3/2) - \Delta E(I = 3/2, m_I = \pm 1/2) \tag{16}$$

where the specific shifts in energy can be calculated as Equation 17,

$$\Delta E = e\alpha(I, m_I)\tilde{Q}\frac{\partial E}{\partial z} \tag{17}$$

where e is the electric charge and α can be described as equation 18.

$$\alpha(I, m_I) = \frac{3m_I^2 - I(I+1)}{I(2I-1)} \tag{18}$$

We can use the difference between the two energy shifts, which we know as ΔE_{quad}, and manipulate Equation 16 to isolate the electric field gradient as in Equation 19.

$$\frac{\partial E}{\partial z} = 4\frac{\Delta E_{quad}}{e}\frac{1}{\tilde{Q}}[\alpha(I = 3/2, m_I = \pm 3/2) - \alpha(I = 3/2, m_I = \pm 1/2)]^{-1} \tag{19}$$

We can then plug in the values for the α equations, the electric charge, the measured ΔE_{quad}, and estimate $\tilde{Q} \approx 0.5$ barns all into Equation 19 to estimate the electric field gradient as $(3.21 \pm 0.03)10^{21} V/m^2$. The uncertainty in this value just comes from the uncertainty in ΔE_{quad} and is described in Equation 20, as e and each α is a well defined value and $\tilde{Q}$ is estimated without uncertainty.

$$d(\frac{\partial E}{\partial z}) = \frac{\partial E}{\partial z}\frac{\Delta(\Delta E_{quad})}{\Delta E_{quad}} \tag{20}$$

6 Conclusion

From the analysis, we find the results as pretty reasonable. For all peaks in the three distributions, each Lorentzian had good fitting parameters with reasonable reduced chi squared values. For the Stainless Steel 302 absorber, we found the mean lifetime as 71.44 ± 5.95 ns, which is outside of uncertainty from the literature value, but still within an order of magnitude. For the Enriched Iron absorber, we found a magnetic field of 32.69 ± 0.10 Teslas, which is within the uncertainty of the literature value. The ratio of μ_0/μ_1 was found to be 0.585 ± 0.002, which is also within uncertainty of the literature value. For the Sodium Nitroprusside absorber, we found an electric field gradient of $(3.21 \pm 0.03)10^{21} V/m^2$, which is expected to be quite large. The mean lifetime measured for each of the peaks in the Enriched Iron and Sodium Nitroprusside Spectrum were all close to each other, and within an order of magnitude of the literature value. For the most part, the findings of this experiment agree with the expected literature values.